

Near-trench coupling conditions offshore the Nicoya Peninsula, Costa Rica and Southern Nicaragua

Mitchell Scott Hastings¹, Eric O. Lindsey², Timothy H Dixon¹, and Surui Xie³

¹University of South Florida

²The University of New Mexico

³University of Houston

November 22, 2022

Abstract

Subduction zone tsunamis require significant co-seismic slip in the shallow, offshore plate interface near the trench, possibly related to the degree of prior interseismic coupling. In Nicaragua, a large tsunami was associated with the 1992 M_w 7.7 earthquake. To the south, the 2012 M_w 7.6 earthquake in the Nicoya peninsula of Costa Rica did not generate a tsunami. The disparate behavior between these two adjacent segments of the Central American megathrust remains unexplained. A stress-constrained model of slip deficit applied to the interseismic surface velocity field in Nicoya suggests a slip deficit rate in the updip portion of the megathrust between 0.8-8.5 cm/yr, suggesting that large tsunamis are possible here. Limited GPS data in Nicaragua can be reconciled by an offshore locked zone that matches the shallow rupture defined by the model of the 1992 tsunami. Sea-floor geodesy would allow much better near-trench constraints on slip deficit in both regions.

Hosted file

cr_supplementary.docx available at <https://authorea.com/users/537703/articles/599992-near-trench-coupling-conditions-offshore-the-nicoya-peninsula-costa-rica-and-southern-nicaragua>

1 **Near-trench coupling conditions offshore the Nicoya**
2 **Peninsula, Costa Rica and Southern Nicaragua**

3 **M. S. Hastings¹, E. O. Lindsey², T. H. Dixon¹, S. Xie³**

4 ¹University of South Florida, School of Geosciences

5 ²University of New Mexico, Earth & Planetary Sciences

6 ³University of Houston, Department of Civil and Environmental Engineering

7 **Key Points:**

- 8 • Large earthquakes occur offshore Nicaragua and generate tsunamis; similar size
9 earthquakes in northern Costa Rica do not.
- 10 • Stress-constrained coupling models for Costa Rica suggest some shallow locking;
11 Seismicity and GPS data in Nicaragua suggest shallow locking is possible.
- 12 • Sea-floor geodesy is necessary to better constrain conditions on the shallow megath-
13 rust in both regions.

Corresponding author: Mitchell Hastings, mshastings1@usf.edu

Abstract

Subduction zone tsunamis require significant co-seismic slip in the shallow, offshore plate interface near the trench, possibly related to the degree of prior interseismic coupling. In Nicaragua, a large tsunami was associated with the 1992 M_w 7.7 earthquake. To the south, the 2012 M_w 7.6 earthquake in the Nicoya peninsula of Costa Rica did not generate a tsunami. The disparate behavior between these two adjacent segments of the Central American megathrust remains unexplained. A stress-constrained model of slip deficit applied to the interseismic surface velocity field in Nicoya suggests a slip deficit rate in the updip portion of the megathrust between 0.8 – 8.5 cm/yr, suggesting that large tsunamis are possible here. Limited GPS data in Nicaragua can be reconciled by an offshore locked zone that matches the shallow rupture model of the 1992 tsunami. Sea-floor geodesy would allow much better near-trench constraints on slip deficit in both regions.

Plain Language Summary

Places where an oceanic plate converges and dives below another plate (continental or oceanic) host the largest earthquakes on Earth. Some but not all of these earthquakes cause catastrophic tsunamis. In the time between earthquakes, part of the sloping boundary between the two plates (the plate interface) is ‘stuck,’ deforming the Earth’s crust. This deformation can be measured at the surface and used to infer motion on the interface. Along the western coast of Central America, the Cocos plate dives beneath the Caribbean plate. The region experiences frequent large earthquakes. Occasional tsunamis occur offshore Nicaragua but not Costa Rica. We use GPS data in the two regions to estimate the amount of motion on the shallow interface close to the sea floor. The data suggest that tsunamis represent a future hazard to both regions.

1 Introduction

One of the challenges in subduction zone hazard assessment is understanding whether a large or great earthquake will be accompanied by a catastrophic tsunami. Attempts have been made to investigate shallow, up-dip locking near the trench using existing on-land GPS, however, they have been unable to determine if that region is fully coupled or freely slipping (Schmalzle et al., 2014; Li et al., 2018). Sea-floor geodetics such as absolute pressure gauges (APGs) and GPS-acoustic (GPS-A) systems have made substantial strides in identifying and constraining shallow locking, but are expensive and difficult to implement and interpret (Bürgmann & Chadwell, 2014; Wallace et al., 2016; Yokota et al., 2016).

The Cocos plate subducts beneath the Caribbean plate at a rate of ~ 84 mm/yr with slight obliquity (DeMets, 2001; DeMets et al., 2010). Historically, the resulting subduction zone offshore Central America has hosted frequent $M \sim 7.2-7.8$ earthquakes with relatively short recurrence intervals, less than 100 years (Figure 1) (Satake, 1994; Protti et al., 1995). Slow slip events (SSEs) are also known here, releasing some fraction of accumulated strain in an aseismic or weakly seismic manner, often accompanied by low frequency earthquakes and non-volcanic seismic tremor (Xie et al., 2020). The region offshore Nicaragua hosted a M_w 7.7 earthquake that generated a tsunami in 1992, causing considerable damage whereas the 2012 M_w 7.6 offshore the Nicoya Peninsula did not generate any tsunamis (Satake, 1994; Norabuena et al., 2004; Dixon et al., 2014; Protti et al., 2014). The megathrust offshore Nicaragua also experiences many more moderate sized earthquakes compared to Nicoya (Figure 2), suggesting contrasts in frictional behavior between these two regions. In this paper, we use available geodetic data and a kinematic coupling model with a stress constraint to investigate the possibility of shallow, up-dip locking in these regions. For the Nicoya Peninsula of northern Costa Rica, with relatively dense geodetic coverage, we estimate a strain budget for the megathrust incorporating strain release via SSEs, and discuss implications for tsunami hazard assessment. Previous work indicates that the coupled regions offshore Nicoya extend to at least 10 km depth (Protti et al., 2014), but our models suggest that the coupled region extends to at least 5 km depth and potentially up to the trench.

2 GPS Data

In northern Costa Rica, we use the data from Xie et al. (2020) to compute interseismic and inter-SSE velocities for the periods before and after the M_w 7.6 5 September 2012 earthquake. The catalog spans July 2002 to July 2020 and contains ten cycles of SSEs. Pre- and post-earthquake locking patterns are remarkably similar, but the post-earthquake period has more stations.

In Nicaragua, we use GPS data processed by the University of Nevada, Reno (Blewitt et al., 2018), and model the GPS time series in the same way as the Costa Rican network, a linear regression with annual/semiannual signals and step-functions for station changes and earthquakes. Some of these stations are located on volcanoes and their signals may be contaminated by local volcanic effects. Several stations have short time spans (~ 1.5 years) and have large uncertainties on the interseismic velocities. One station, CN22, is located in a residential area of the coastal town of PoneLOYA, Nicaragua and displays mostly western motion, possibly indicating contamination by other sources of deformation.

Both the Costa Rican and Nicaraguan site velocity data exhibit significant northwest components associated with trench-parallel forearc block motion (Figure 3) (McCaffrey et al., 2002; DeMets, 2001; Norabuena et al., 2004; Turner et al., 2007; LaFemina et al., 2009). For the velocity of the subducted plate, we used the PVEL model (DeMets et al., 2010). Misfits between the predictions of this model and the observed GPS velocity at

88 Cocos Island (Protti et al., 2012) suggest that PVEL may be slightly biased, but the dif-
 89 ferences are not significant for purposes of our model. Since both Nicoya and southern
 90 Nicaragua experience motion of a forearc sliver block, we calculated the effective rake
 91 direction and rate on the subduction interface assuming 10 mm/yr of northwest block
 92 motion for Nicoya, and 15 mm/yr of northwest block motion for southern Nicaragua. The
 93 corresponding rake direction differs little from the predicted PVEL direction of motion,
 94 hence simply taking the component of motion for a given site velocity in the PVEL di-
 95 rection is an adequate approximation.

96 **3 Kinematic Coupling Models offshore Northern Costa Rica**

97 We divide the megathrust into discrete triangular patches following the Slab 2.0
 98 plate interface (Hayes et al., 2018) and apply a new kinematic coupling model with stress-
 99 constraints on the fault patches (Lindsey et al., 2021). This model uses a boundary el-
 100 element method to apply analytical solutions for displacements and stressing rate in an
 101 elastic half space. The model imposes a non-zero stressing rate via the stress interaction
 102 kernel that acts as a physics-based minimum smoothness constraint. This stress kernel
 103 is constructed by evaluating the effect of the slip vector on each patch for all the patches.
 104 Thus, the smoothing effect of the stress-constraint is highest for regions that are up-dip
 105 of highly coupled patches. There is an additional Laplacian smoothing parameter within
 106 the model that does not exploit physics for a more variable smoothing effect. For that
 107 parameter, we use an L-curve approach and compute the point of maximum curvature
 108 to select an optimal smoothing parameter.

109 We used two types of priors (maximum and minimum coupling) to estimate the
 110 range of possible coupling behavior for the Central American megathrust. The priors are
 111 implemented by imposing a penalty on the total slip rate deficit. This is calculated by
 112 summing the slip rates on all the patches and penalizing the difference between that sum
 113 and either zero (minimum coupling) or the long-term slip rate (maximum coupling). The
 114 inversion is iterated over a range of reasonable penalty parameters for both the minimum
 115 and maximum solution, which allows tracking of the minimum and maximum allowable
 116 coupling values on each patch. The variance in the physical domain is defined by the dif-
 117 ference between the maximum and minimum coupling values at each patch, and we use
 118 this as a metric for model resolution as well as computing model uncertainty. When the
 119 penalty parameter is zero there is no difference between the maximum and minimum so-
 120 lutions; this is the best-fitting model.

121 Our preferred model uses the interseismic velocities from the post-2012 period (Fig-
 122 ure 4a). Regardless of the penalty parameter, all models show a highly coupled patch
 123 underneath the center of the Nicoya Peninsula and another highly coupled patch to the
 124 east beneath the Gulf of Nicoya. Increasing the penalty parameter on the minimum cou-
 125 pling inversion reduces the coupling around these two high-coupled patches and even-
 126 tually, with a large enough parameter, the two main patches converge into one patch be-
 127 neath the southeastern region of Nicoya. Conversely, increasing the penalty parameter
 128 on the maximum coupling inversion reduces the degree of coupling around these patches
 129 forcing increased coupling away from the data. The minimum coupling inversions tend
 130 to fit the data better than the maximum coupling inversions (i.e. the same penalty pa-
 131 rameter yields a better fit in the minimum inversion compared to the maximum).

132 We also investigated interseismic velocities from the pre-2012 period. There is sig-
 133 nificant overlap in the coupling patches of both periods (Figure 4). For the pre-2012 model,
 134 the central patch is located farther offshore, and shows a highly-coupled region at about
 135 35 km depth in the northwest region of Nicoya, consistent with modeled slow slip in 2009,
 136 2011, and 2014 (Xie et al., 2020). Both models show strong correlation with the rupture
 137 zone of the 2012 Costa Rica earthquake (Figure 1 and 2), as well as deep slow slip (~ 40 km)
 138 beneath the Gulf of Nicoya.

139 All of the models (pre- and post-2012) indicate a high degree of variance in the near-
 140 trench portion of the subduction zone, with the maximum coupling close to the full plate
 141 rate. Figure 5 shows the minimum and maximum coupling on each patch over the range
 142 of solutions for the post-2012 period and a transect perpendicular to the trench. The cou-
 143 pling is well-constrained in the region of the 2012 rupture zone between 40–70% with
 144 the best-fit values being between 50–60% coupled for both the pre- and post-2012 pe-
 145 riods. Figure 5c also compares the coupling values to strain release processes associated
 146 with this section of the megathrust (coseismic ruptures, postseismic slip, and SSEs). Large
 147 earthquakes and SSEs apparently release most of the accumulated strain in the deeper
 148 parts of the subduction zone, but do not fully accommodate the shallow strain. At the
 149 trench, the variability ranges from a minimum of 15% up to $\sim 98\%$, effectively full cou-
 150 pling. This variability is also seen in adjacent sections of the trench (Figure 6).

151 4 Forward Locking Models offshore Southern Nicaragua

152 The GPS network in Nicaragua is not sufficiently dense nor close enough to the trench
 153 to apply the coupling model reliably. However, with some assumptions, useful informa-
 154 tion about the frictional behavior of the megathrust can be obtained from simple for-
 155 ward models. We tested whether the tsunami or seismological/aftershock models of the
 156 1992 M_w 7.7 earthquake are consistent with the available GPS data, assuming that the
 157 rupture zone for that event is also the zone that is currently fully locked.

158 We modeled the interseismic velocities in Nicaragua with a range of locking mod-
 159 els in the shallow megathrust (Okada, 1992). Seismological models, based on aftershock
 160 distribution, tend to favor large rupture zones with significant down-dip extent (Ide et
 161 al., 1993; Norabuena et al., 2004). These models are not consistent with the current GPS
 162 velocity field. Figure 7 shows a range of locking models and the tsunami rupture model
 163 of Satake (1994). The GPS locking model and the tsunami rupture model both imply
 164 a limited depth down-dip extent of locking/rupture, $\sim 40 - 50$ km, at a depth of ap-
 165 proximately 20 – 25 km on the plate interface.

166 5 Discussion

167 The tsunami record in Costa Rica dates back to 1579 and includes 14 events re-
 168 lated to earthquakes (NOAA, 2020). The tsunami associated with the M_w 7.6 1991 Limón
 169 earthquake is the only significant event recorded with wave heights of $\sim 2-3$ m. How-
 170 ever, this earthquake and tsunami occurred on the Caribbean side of Costa Rica and are
 171 unrelated to the subduction megathrust. All other tsunamis in Costa Rica have been small,
 172 with 10 – 30 cm wave heights.

173 The megathrust offshore the Nicoya Peninsula in northwest Costa Rica hosts earth-
 174 quakes of order M_w 7.5 with a recurrence interval of 50–60 years (Protti et al., 2014),
 175 but there are no recorded tsunamis associated with these events. In contrast, areas in
 176 Central America northwest of Costa Rica do host significant tsunamis. In 1992, a M_w
 177 7.7 earthquake offshore Nicaragua generated a tsunami with ~ 10 m waves that killed
 178 at least 168 people and left 13,500 homeless (Kanamori & Kikuchi, 1993; Satake, 1994;
 179 Kikuchi & Kanamori, 1995; Satake, 1995). In 2003, a M_w 7.3 megathrust earthquake
 180 in El Salvador near the Gulf of Fonseca created a tsunami with ~ 6.3 m wave heights (Heidarzadeh
 181 & Satake, 2014).

182 The contrast in recent and historical tsunami behavior between these two adjacent
 183 sections of the Central American subduction zone raises an obvious question. Are large
 184 tsunamis offshore Costa Rica not possible, or is the tsunami/earthquake record simply
 185 too short to have observed these events? In other words, is there a fundamental differ-
 186 ence in the properties of the subduction megathrust that limits tsunami risk offshore Costa
 187 Rica, versus megathrust properties to the north that promote tsunamis?

188 The record length for Costa Rica (~ 450 year) is long enough to suggest the differ-
 189 ence in tsunami recurrence between two areas is significant. Perhaps the absence of tsunamis
 190 in Costa Rica reflects a lack of strain accumulation in the shallow megathrust here; data
 191 from the current on-shore geodetic network are not diagnostic as they lacks sensitivity
 192 to strain accumulation near the trench. Our new kinematic strain accumulation model,
 193 accounting for realistic stress shadow effects, provide some constraints and suggests that
 194 strain may indeed be accumulating in this up-dip region but uncertainties remain large.
 195 Jiang et al. (2017) documented an elastic strain release event in the shallow megathrust
 196 offshore Nicoya, suggesting prior strain accumulation here.

197 If up-dip strain had indeed accumulated here, why was it not released in the 2012
 198 earthquake? Recent models of earthquake 'super-cycles' suggest that strain can accu-
 199 mulate over many earthquake cycles, i.e. all accumulated strain is not necessarily released
 200 in a given event (Sieh et al., 2008; Salditch et al., 2020). It has also been shown that large
 201 earthquakes tend to cluster in time (Kulkarni et al., 2013; Goldfinger et al., 2013), con-
 202 sistent with the idea of temporal variation of strain accumulation/release. If these con-
 203 cepts apply to Costa Rica, it is possible that long-term strain is accumulating near the
 204 trench and could contribute to a large tsunami in the future.

205 The coupling model from Protti et al. (2014) suggests that there is a fully coupled
 206 area along the coast of the Nicoya Peninsula that did not rupture during the 2012 earth-
 207 quake. Our models suggest that this region is $\sim 40\%$ coupled and accruing $\sim 3-3.5$ cm/yr
 208 of slip. This region also experiences SSEs approximately every two years and releases
 209 about 1.5–2 cm of strain (Voss et al., 2017; Xie et al., 2020; Afra et al., submitted to
 210 JGR). This suggests that this area may be accumulating strain more slowly than pre-
 211 viously thought and perhaps explains why it did not participate in the 2012 rupture, though
 212 this does not preclude it from participating in future great earthquakes.

213 The slip rate deficit at the trench estimated by our models is between 10 – 95%
 214 of the plate rate ($\sim 0.85-8.5$ cm/yr) (Figure 5c). Hence, the potential strain accumu-
 215 lation offshore Costa Rica is of order $\sim 4-35$ m based on the 450 year record of no tsunamis.
 216 While this maximum value seems extreme, we note that even higher strain release was
 217 observed in Japan during the 2011 M_w 9.0 Tohoku-Oki earthquake. Prior to that event,
 218 the up-dip region of the seismogenic zone had been considered aseismic (velocity strength-
 219 ening), incapable of hosting rapid seismic slip. In the event, the earthquake caused up
 220 to ~ 50 m of offset at the trench (Kimura et al., 2012). Before the 2011 Tohoku-Oki event,
 221 the megathrust had a prior history of recurring $M \sim 7$ earthquakes (1915, 1962, 1980,
 222 2003) (Uchida & Bürgmann, 2021). The potential similarity with the Costa Rican record
 223 suggests to us that tsunami hazard estimates in this part of Central America based only
 224 on the historical record could be under-estimated, despite that record's 450-year length.

225 The forward locking models offshore Southern Nicaragua are consistent with the
 226 tsunami model proposed by Satake (1994), but due to the uncertainties on the interseis-
 227 mic velocities it is difficult to estimate anything more than the down-dip extent of lock-
 228 ing. The down-dip extent is consistent with shallow locking and our models rule out deep
 229 locking offshore Nicaragua (Figure 8). Sea-floor geodetic data would help to better con-
 230 strain the down-dip extent and more localized regions of locking.

231 Assuming the tsunami rupture model accurately outlines the current locking pat-
 232 tern, as suggested by the limited GPS data, there is a spatial correlation between lock-
 233 ing and bathymetric depth. The steep gradient in near-trench bathymetry, from about
 234 4,000 meters to less than 500 meters within 45 km of the trench, closely matches the re-
 235 gion we infer to be presently locked. Perhaps this locked zone persists over many seis-
 236 mic cycles, promoting back-thrusts that locally steepen and thicken the crust. Xie et al.
 237 (2020) noted the similarity between pre- and post-2012 locking patterns in and near the
 238 Nicoya peninsula, also consistent with longer term persistence in locking patterns.

239 There were over 250 moderate earthquakes ($M_w 5 - 6.9$) between 1976 and 2022
 240 offshore Southern Nicaragua and Northern Costa Rica (Figure 2). Prior to the 1992 event,
 241 seismicity is sparsely distributed offshore Nicaragua. After the 1992 event two major clusters
 242 of seismicity occur offshore Nicaragua, southeast and northwest of the hypocenter.
 243 These high-density clusters largely overlap with the locking zone inferred from the geode-
 244 tic data.

245 Three normal-faulting earthquakes occurred in the outer-rise in the year after the
 246 1992 Nicaragua earthquake. These types of earthquakes have been interpreted to indi-
 247 cate prior shallow locking, with the subsequent large megathrust earthquake stimulat-
 248 ing extension in the outer-rise (Sladen & Trevisan, 2018). Offshore Nicoya there are not
 249 as many clear indicators of shallow locking such as the high-volume of earthquakes near
 250 the trench or large tsunami run-ups. Though there are fewer outer-rise earthquakes, there
 251 are two prior to the 2012 earthquake and one after 2013, all greater than $M_w 5.0$.

252 The available tsunami, seismic, and geodetic data in Nicaragua are in agreement
 253 that the near-trench region is locked and can generate tsunamis. Assuming locking con-
 254 tinues, at the full plate rate, this portion of the subduction zone will reach 3 meters of
 255 accumulated strain (the amount released in the 1992 earthquake) within the next 1–
 256 3 decades.

257 6 Conclusions

- 258 • A stress-constrained kinematic coupling model for the interseismic surface veloc-
 259 ity field in northern Costa Rica predicts a locked (slip deficit) zone that agrees with
 260 the rupture zone of the 2012 $M_w 7.6$ Costa Rica earthquake. The model suggests
 261 the offshore region experiences slip deficit at 10–95% of the full plate rate, with
 262 25% as the best estimate. The potential therefore exists for a major tsunami here,
 263 despite a 450-year tsunami-free record.
- 264 • The GPS surface velocity field in Nicaragua is consistent with a shallow locking
 265 model that resembles the 1992 tsunami rupture model of Satake (1994).
- 266 • If the shallow megathrust offshore Nicaragua remains fully locked, as implied by
 267 the limited GPS data, there is potential for another large earthquake and tsunami
 268 within the next 1-3 decades.
- 269 • Sea-floor geodesy would significantly improve our ability to constrain locking on
 270 the shallow megathrust in both Nicaragua and Costa Rica.

271 7 Acknowledgments

272 This research was partially supported by the National Science Foundation grants
 273 1835947 to T. H. D. Special thanks to Emile Okal for referring us to the NOAA tsunami
 274 database. We would also like to thank Jochen Braunmiller for reviewing and challeng-
 275 ing our models throughout the process.

276 **References**

- 277 Afra, M., Hastings, M. S., Xie, S., Chaves, E., Muller, C., Protti, M., ... Alvarez-
 278 Calderón, A. (submitted to JGR). Slow slip prior to an earthquake: An
 279 example from costa rica and forecasting implications. *Journal of Geophysical*
 280 *Research: Solid Earth*.
- 281 Blewitt, G., Hammond, W. C., & Kreemer, C. (2018). Harnessing the gps data ex-
 282 plosion for interdisciplinary science. *Eos*, *99*(10.1029), 485.
- 283 Bürgmann, R., & Chadwell, D. (2014). Seafloor geodesy. *Annual Review of Earth*
 284 *and Planetary Sciences*, *42*, 509–534.
- 285 DeMets, C. (2001). A new estimate for present-day cocos-caribbean plate motion:
 286 Implications for slip along the central american volcanic arc. *Geophysical re-*
 287 *search letters*, *28*(21), 4043–4046.
- 288 DeMets, C., Gordon, R. G., & Argus, D. F. (2010). Geologically current plate mo-
 289 tions. *Geophysical journal international*, *181*(1), 1–80.
- 290 Dixon, T. H., Jiang, Y., Malservisi, R., McCaffrey, R., Voss, N., Protti, M., & Gon-
 291 zalez, V. (2014). Earthquake and tsunami forecasts: Relation of slow slip
 292 events to subsequent earthquake rupture. *Proceedings of the National Academy*
 293 *of Sciences*, *111*(48), 17039–17044.
- 294 Dziewonski, A. M., Chou, T.-A., & Woodhouse, J. H. (1981). Determination of
 295 earthquake source parameters from waveform data for studies of global and
 296 regional seismicity. *Journal of Geophysical Research: Solid Earth*, *86*(B4),
 297 2825–2852.
- 298 Goldfinger, C., Ikeda, Y., Yeats, R. S., & Ren, J. (2013). Superquakes and supercy-
 299 cles. *Seismological Research Letters*, *84*(1), 24–32.
- 300 Hayes, G. P., Moore, G. L., Portner, D. E., Hearne, M., Flamme, H., Furtney, M.,
 301 & Smoczyk, G. M. (2018). Slab2, a comprehensive subduction zone geometry
 302 model. *Science*, *362*(6410), 58–61.
- 303 Heidarzadeh, M., & Satake, K. (2014). The el salvador and philippines tsunamis
 304 of august 2012: insights from sea level data analysis and numerical modeling.
 305 *Pure and Applied Geophysics*, *171*(12), 3437–3455.
- 306 Ide, S., Imamura, F., Yoshida, Y., & Abe, K. (1993). Source characteristics of the
 307 nicaraguan tsunami earthquake of september 2, 1992. *Geophysical research let-*
 308 *ters*, *20*(9), 863–866.
- 309 Jiang, Y., Liu, Z., Davis, E. E., Schwartz, S. Y., Dixon, T. H., Voss, N., ... Protti,
 310 M. (2017). Strain release at the trench during shallow slow slip: The ex-
 311 ample of nicoya peninsula, costa rica. *Geophysical Research Letters*, *44*(10),
 312 4846–4854.
- 313 Kanamori, H., & Kikuchi, M. (1993). The 1992 nicaragua earthquake: a slow
 314 tsunami earthquake associated with subducted sediments. *Nature*, *361*(6414),
 315 714–716.
- 316 Kikuchi, M., & Kanamori, H. (1995). Source characteristics of the 1992 nicaragua
 317 tsunami earthquake inferred from teleseismic body waves. In *Tsunamis: 1992–*
 318 *1994* (pp. 441–453). Springer.
- 319 Kimura, G., Hina, S., Hamada, Y., Kameda, J., Tsuji, T., Kinoshita, M., & Ya-
 320 maguchi, A. (2012). Runaway slip to the trench due to rupture of highly
 321 pressurized megathrust beneath the middle trench slope: the tsunamigenesis
 322 of the 2011 tohoku earthquake off the east coast of northern japan. *Earth and*
 323 *Planetary Science Letters*, *339*, 32–45.
- 324 Kulkarni, R., Wong, I., Zachariassen, J., Goldfinger, C., & Lawrence, M. (2013). Sta-
 325 tistical analyses of great earthquake recurrence along the cascadia subduction
 326 zone. *Bulletin of the Seismological Society of America*, *103*(6), 3205–3221.
- 327 LaFemina, P., Dixon, T. H., Govers, R., Norabuena, E., Turner, H., Saballos, A.,
 328 ... Strauch, W. (2009). Fore-arc motion and cocos ridge collision in central
 329 america. *Geochemistry, Geophysics, Geosystems*, *10*(5).

- 330 Li, S., Wang, K., Wang, Y., Jiang, Y., & Dosso, S. E. (2018). Geodetically inferred
 331 locking state of the cascadia megathrust based on a viscoelastic earth model.
 332 *Journal of Geophysical Research: Solid Earth*, *123*(9), 8056–8072.
- 333 Lindsey, E. O., Mallick, R., Hubbard, J. A., Bradley, K. E., Almeida, R. V., Moore,
 334 J. D., ... Hill, E. M. (2021). Slip rate deficit and earthquake potential on
 335 shallow megathrusts. *Nature Geoscience*, *14*(5), 321–326.
- 336 McCaffrey, R., Stein, S., & Freymueller, J. (2002). Crustal block rotations and plate
 337 coupling. *Plate Boundary Zones, Geodyn. Ser.*, *30*, 101–122.
- 338 NOAA. (2020). National geophysical data center/world data service: Ncei/wds
 339 global historical tsunami database.
- 340 Norabuena, E., Dixon, T. H., Schwartz, S., DeShon, H., Newman, A., Protti, M.,
 341 ... others (2004). Geodetic and seismic constraints on some seismogenic
 342 zone processes in costa rica. *Journal of Geophysical Research: Solid Earth*,
 343 *109*(B11).
- 344 Okada, Y. (1992). Internal deformation due to shear and tensile faults in a half-
 345 space. *Bulletin of the seismological society of America*, *82*(2), 1018–1040.
- 346 Protti, M., González, V., Freymueller, J., & Doelger, S. (2012). Isla del coco,
 347 on cocos plate, converges with isla de san andrés, on the caribbean plate, at
 348 78mm/yr. *Revista de Biología Tropical*, *60*, 33–41.
- 349 Protti, M., González, V., Newman, A. V., Dixon, T. H., Schwartz, S. Y., Marshall,
 350 J. S., ... Owen, S. E. (2014). Nicoya earthquake rupture anticipated by
 351 geodetic measurement of the locked plate interface. *Nature Geoscience*, *7*(2),
 352 117–121.
- 353 Protti, M., McNally, K., Pacheco, J., Gonzalez, V., Montero, C., Segura, J., ...
 354 others (1995). The march 25, 1990 (mw= 7.0, ml= 6.8), earthquake at the
 355 entrance of the nicoya gulf, costa rica: Its prior activity, foreshocks, after-
 356 shocks, and triggered seismicity. *Journal of Geophysical Research: Solid Earth*,
 357 *100*(B10), 20345–20358.
- 358 Salditch, L., Stein, S., Neely, J., Spencer, B. D., Brooks, E. M., Agnon, A., & Liu,
 359 M. (2020). Earthquake supercycles and long-term fault memory. *Tectono-*
 360 *physics*, *774*, 228289.
- 361 Satake, K. (1994). Mechanism of the 1992 nicaragua tsunami earthquake. *Geophysi-*
 362 *cal Research Letters*, *21*(23), 2519–2522.
- 363 Satake, K. (1995). Linear and nonlinear computations of the 1992 nicaragua earth-
 364 quake tsunami. *Pure and Applied Geophysics*, *144*(3), 455–470.
- 365 Schmalzle, G. M., McCaffrey, R., & Creager, K. C. (2014). Central cascadia subduc-
 366 tion zone creep. *Geochemistry, Geophysics, Geosystems*, *15*(4), 1515–1532.
- 367 Sieh, K., Natawidjaja, D. H., Meltzner, A. J., Shen, C.-C., Cheng, H., Li, K.-S., ...
 368 Edwards, R. L. (2008). Earthquake supercycles inferred from sea-level changes
 369 recorded in the corals of west sumatra. *Science*, *322*(5908), 1674–1678.
- 370 Sladen, A., & Trevisan, J. (2018). Shallow megathrust earthquake ruptures betrayed
 371 by their outer-trench aftershocks signature. *Earth and Planetary Science Let-*
 372 *ters*, *483*, 105–113.
- 373 Turner, H. L., LaFemina, P., Saballos, A., Mattioli, G. S., Jansma, P. E., & Dixon,
 374 T. (2007). Kinematics of the nicaraguan forearc from gps geodesy. *Geophysical*
 375 *Research Letters*, *34*(2).
- 376 Uchida, N., & Bürgmann, R. (2021). A decade of lessons learned from the 2011
 377 tohoku-oki earthquake. *Reviews of Geophysics*, *59*(2), e2020RG000713.
- 378 Voss, N. K., Malservisi, R., Dixon, T. H., & Protti, M. (2017). Slow slip events in
 379 the early part of the earthquake cycle. *Journal of Geophysical Research: Solid*
 380 *Earth*, *122*(8), 6773–6786.
- 381 Wallace, L. M., Webb, S. C., Ito, Y., Mochizuki, K., Hino, R., Henrys, S., ... Shee-
 382 han, A. F. (2016). Slow slip near the trench at the hikurangi subduction zone,
 383 new zealand. *Science*, *352*(6286), 701–704.
- 384 Xie, S., Dixon, T. H., Malservisi, R., Jiang, Y., Protti, M., & Muller, C. (2020).

- 385 Slow slip and inter-transient locking on the nicoya megathrust in the late and
386 early stages of an earthquake cycle. *Journal of Geophysical Research: Solid*
387 *Earth*, 125(11), e2020JB020503.
- 388 Yokota, Y., Ishikawa, T., Watanabe, S.-i., Tashiro, T., & Asada, A. (2016). Seafloor
389 geodetic constraints on interplate coupling of the nankai trough megathrust
390 zone. *Nature*, 534(7607), 374–377.
- 391 Yue, H., Lay, T., Schwartz, S. Y., Rivera, L., Protti, M., Dixon, T. H., . . . Newman,
392 A. V. (2013). The 5 september 2012 nicoya, costa rica mw 7.6 earthquake
393 rupture process from joint inversion of high-rate gps, strong-motion, and tele-
394 seismic p wave data and its relationship to adjacent plate boundary interface
395 properties. *Journal of Geophysical Research: Solid Earth*, 118(10), 5453–5466.

8 Figures

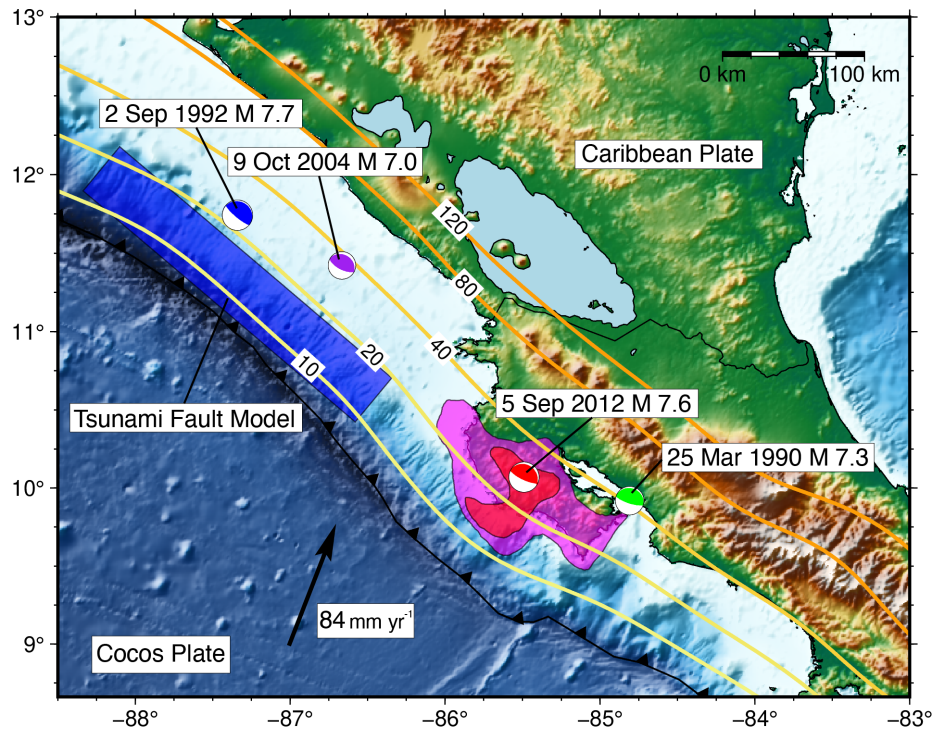


Figure 1. Bathymetry and topography of the study area based on a 30-arc second Digital Elevation Model of Central America, with major earthquakes (USGS) and selected depth contours (in km) on the subducting plate interface. Rupture zone of the 2012 M_w 7.6 Costa Rica earthquake (red patch is the 1.2 meter slip contour of Yue et al. (2013)) and pre-seismic locked zone for the event (magenta patch is the area with coupling ratio greater than 0.3 in coupling model of Protti et al. (2014)) are shown for comparison. Rupture zone of the 1992 M_w 7.7 Nicaragua earthquake (blue rectangle) is inferred from the tsunami fault model of Satake (1994).

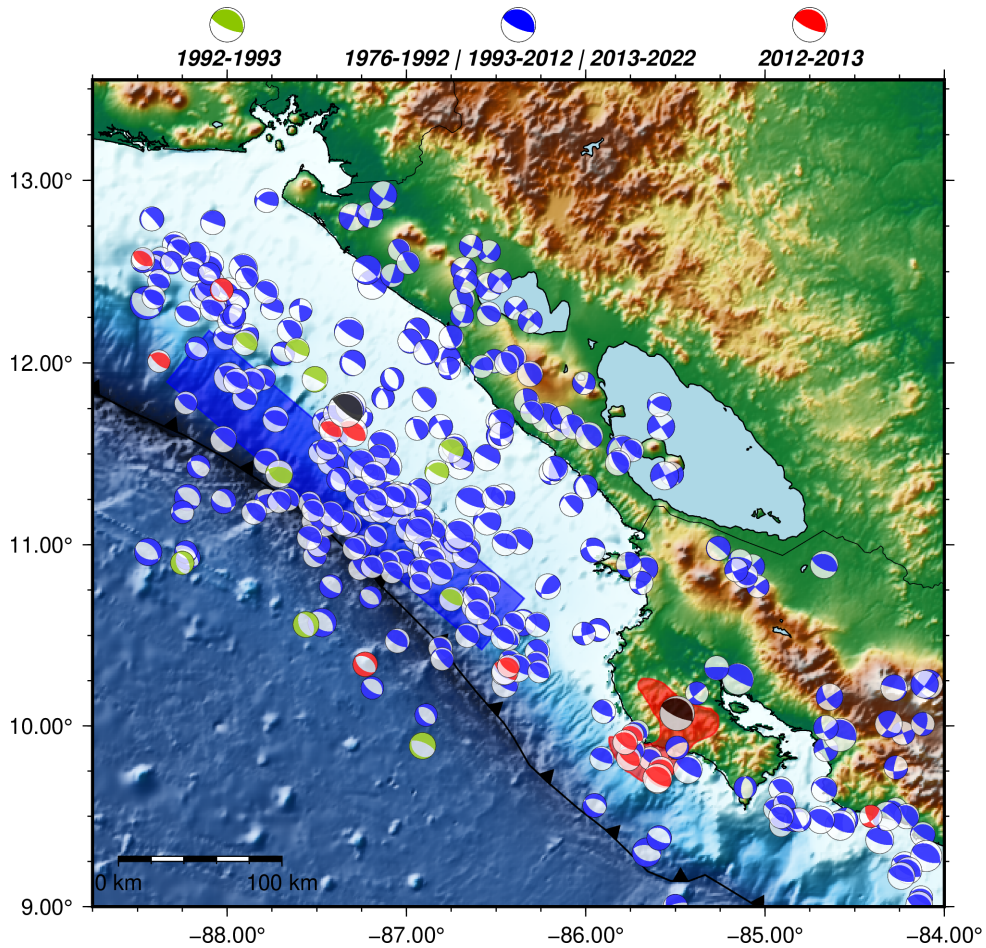


Figure 2. Comparison of earthquake frequency and location offshore northern Costa Rica and Nicaragua, from the Global Centroid Moment Tensor Catalog (Dziewonski et al., 1981). One year aftershocks from the 1992 M_w 7.7 Nicaragua and 2012 M_w 7.6 Costa Rica earthquakes are color-coded, light green and red, respectively.

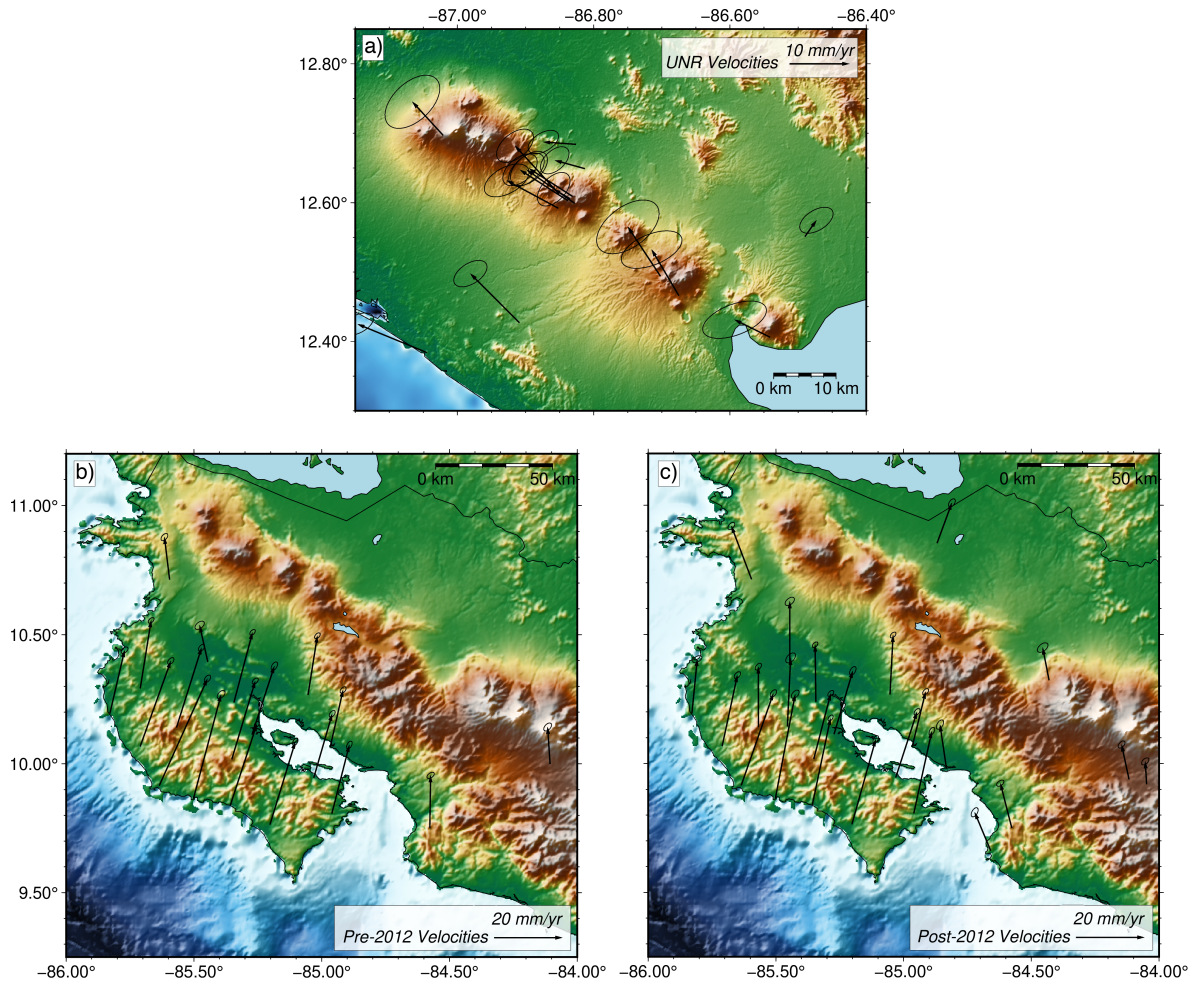


Figure 3. Interseismic surface velocity for (a) Nicaragua (Blewitt et al., 2018) and (b,c) Costa Rica (Xie et al., 2020). Costa Rica data show periods before and after the 2012 M_w 7.6 earthquake. Both periods have similar velocity patterns, reflecting a combination of plate motion-parallel strain accumulation from locking on the megathrust and trench-parallel forearc motion. Nicaragua data, farther from the locked megathrust, are dominated by trench-parallel forearc motion.

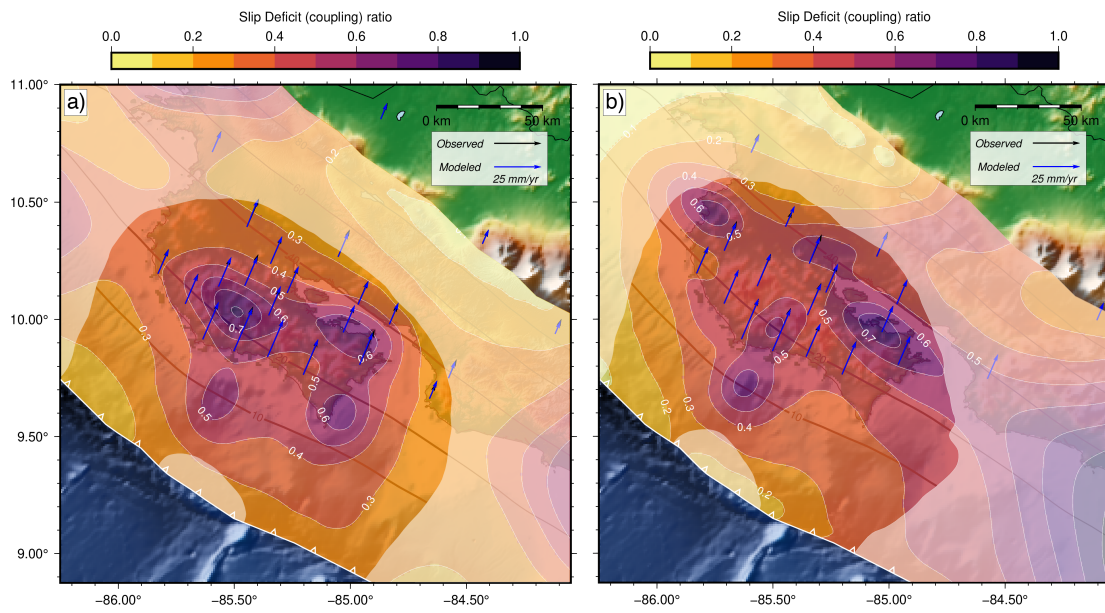


Figure 4. (a) Best-fit kinematic coupling model for northern Costa Rica using plate motion-parallel component of interseismic surface velocities (black arrows are data vectors and blue are model vectors) for the the post-2012 period and the (b) pre-2012 period. The models are overlain on a regional DEM, with more transparent sections indicating poorly constrained regions (see Figure 6). Thin black contours show slab depth from Hayes et al. (2018).

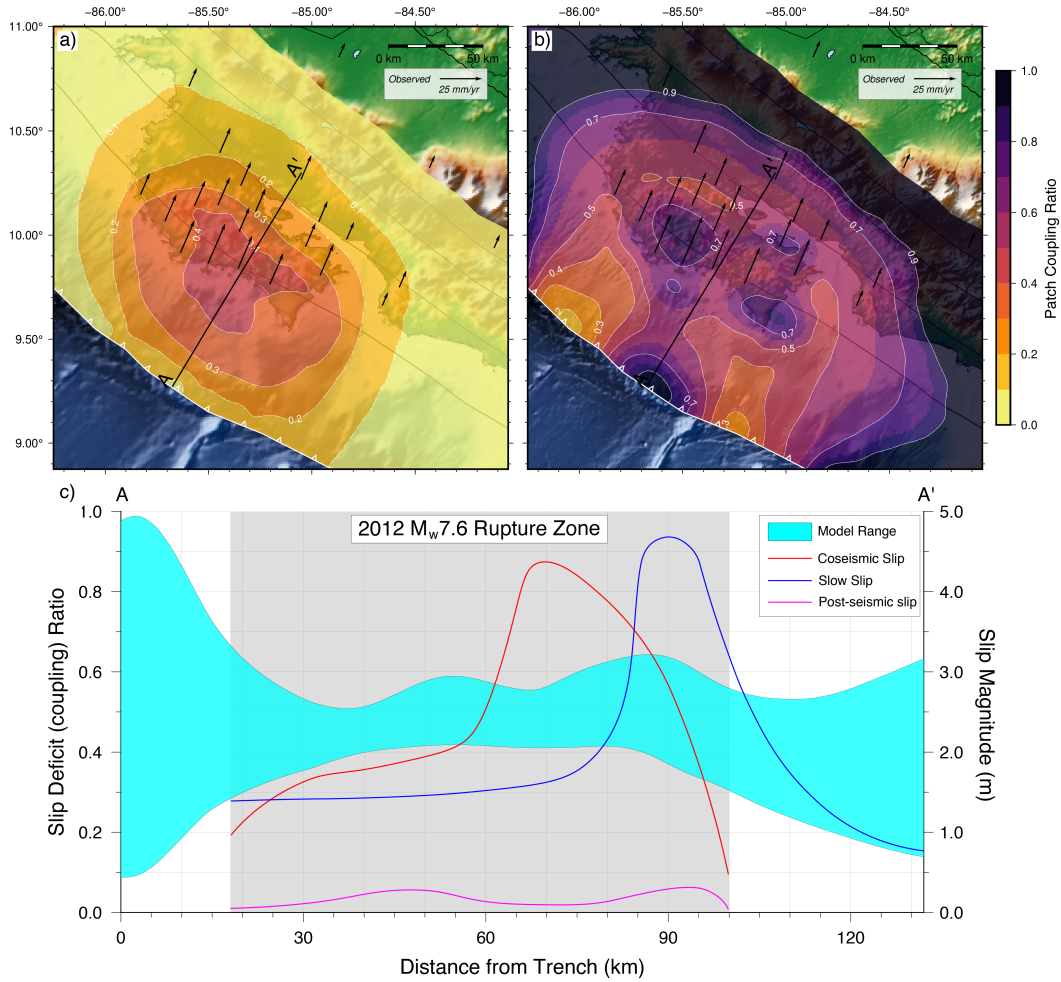


Figure 5. Minimum (a) and maximum (b) coupling ratio for each patch (location) from a range of inversion solutions. Line A-A' shows the location of the trench-perpendicular transect through the rupture zone of the 2012 M_w 7.6 earthquake. (c) Comparison of strain accumulation (slip deficit) along line A-A' and various strain release processes (earthquake rupture, post-seismic slip, and slow slip). Note that a significant fraction of accumulated strain may be unreleased in the offshore region close to the trench, implying that the possibility of a future tsunami, but uncertainties are large due to lack of near-trench observations.

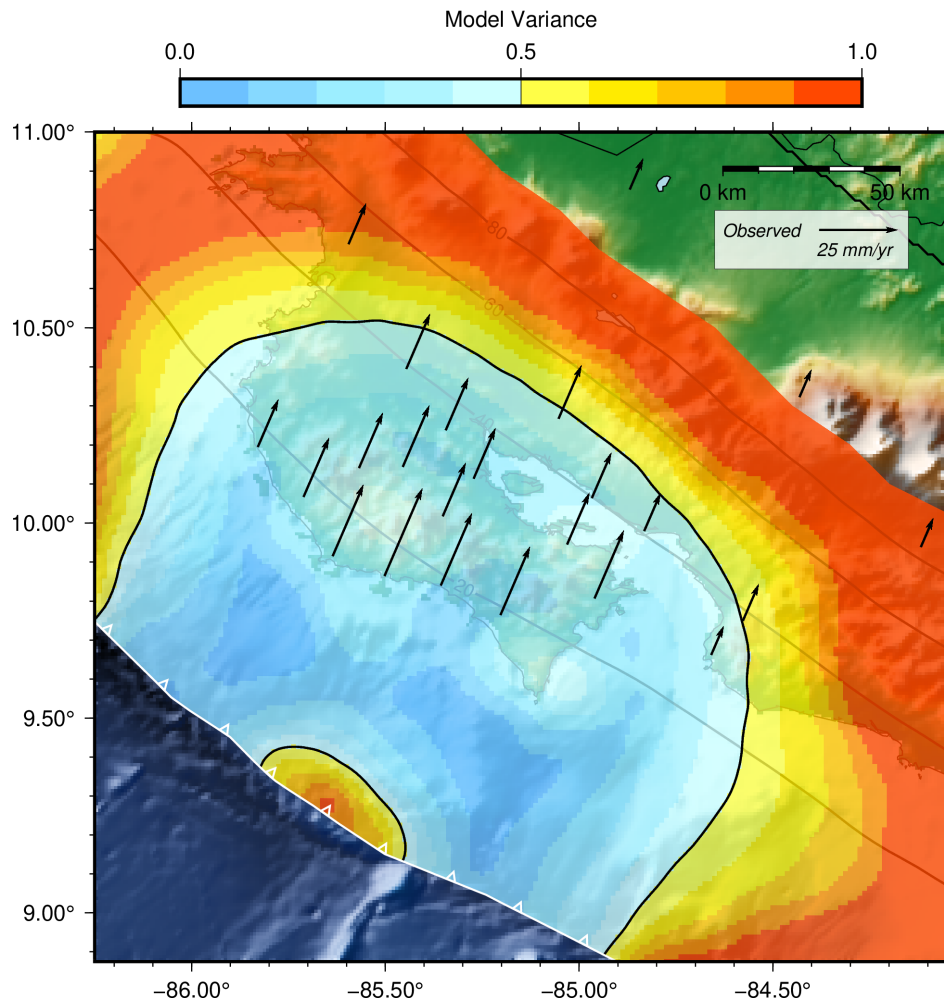


Figure 6. Variance in the coupling ratio for each patch in the model. Values larger than 0.5 are poorly constrained.

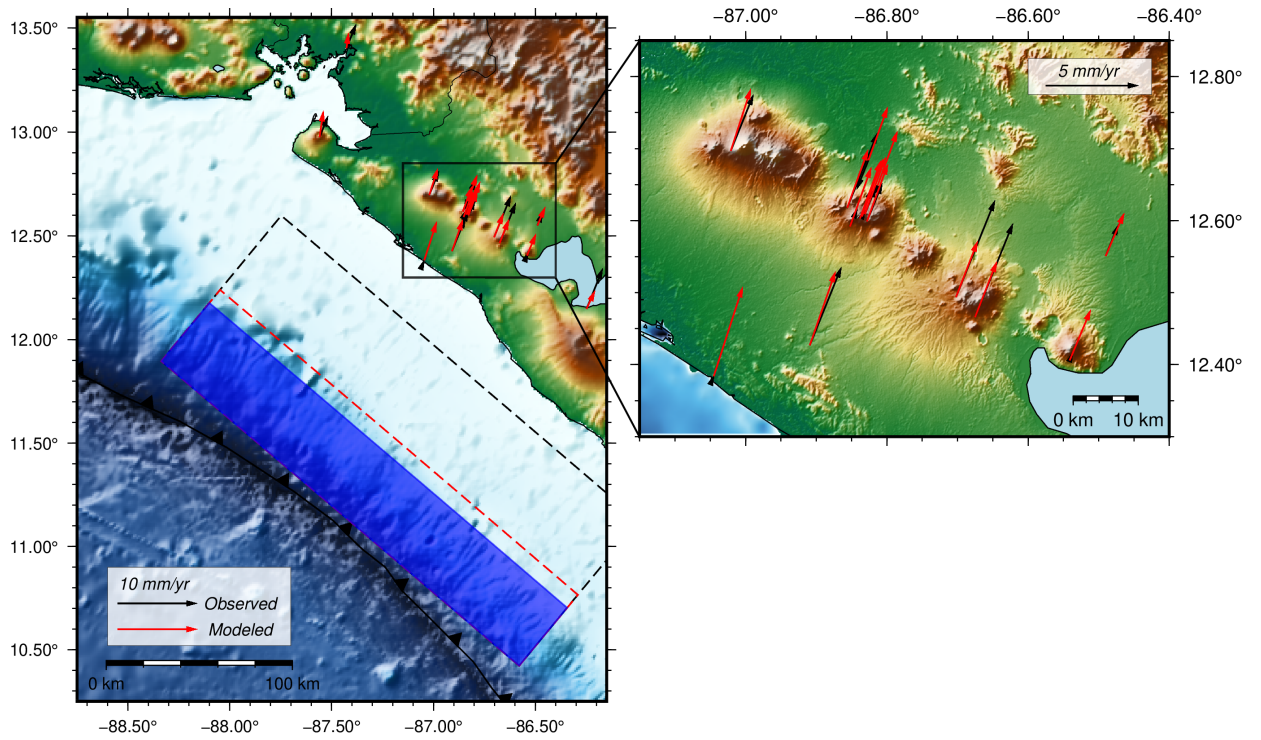


Figure 7. Proposed rupture models for the 1992 M_w 7.7 Nicaragua earthquake based on aftershock distribution (dashed black rectangle; Ide et al. (1993)) and tsunami run-up (blue solid rectangle; Satake (1994)), compared to a GPS-based forward model for locking (red dashed line). Inset shows GPS surface velocity data (black arrows) and predictions from the best-fit forward model (red arrows), which closely matches the tsunami-based rupture model.

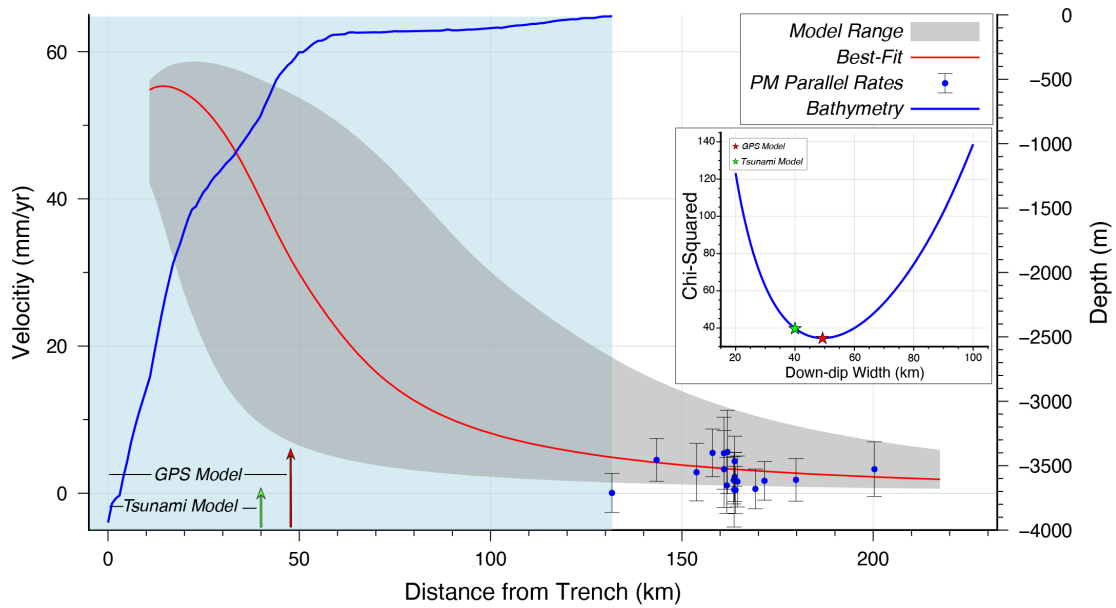


Figure 8. Bathymetric profile offshore Nicaragua compared to surface velocities predicted by the GPS-based locking model in Figure 7. Inset shows the chi-squared error for various depths of maximum locking in the forward model. Note the close agreement between the GPS locking model and the tsunami rupture model. While the on-shore GPS data are far from the locked zone, they can at least rule out the deeper down-dip width implied by the seismological model in Figure 7 assuming current locking matches the 1992 rupture.